Volume 3 | Number 43 | 21 November 2015 | Pages 11259–11556

Journal of Materials Chemistry C

Materials for optical, magnetic and electronic devices

www.rsc.org/MaterialsC

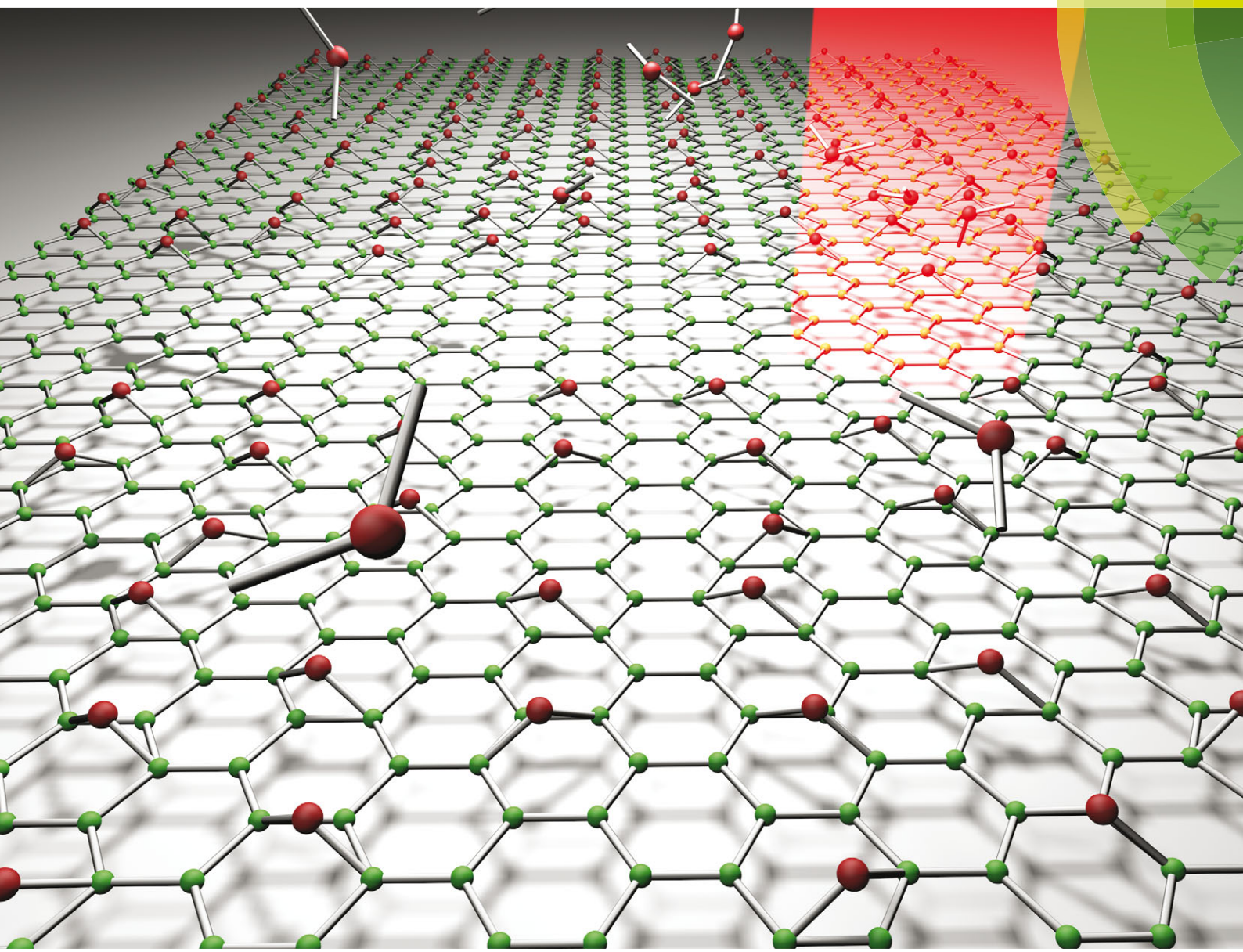

ISSN 2050-7526

ROYAL SOCIETY OF CHEMISTRY

PAPER

Winco K. C. Yung, Guijun Li, Hang Shan Choy, Zhixiang Cai *et al.*
Eye-friendly reduced graphene oxide circuits with nonlinear optical transparency on flexible poly(ethylene terephthalate) substrates

Journal of Materials Chemistry C

PAPER

View Article Online
View Journal | View Issue

Cite this: J. Mater. Chem. C, 2015, 3, 11294

Eye-friendly reduced graphene oxide circuits with nonlinear optical transparency on flexible poly(ethylene terephthalate) substrates

Winco K. C. Yung, Guijun Li,* Hai Ming Liem, Hang Shan Choy and Zhixiang Cai

Received 4th August 2015,
Accepted 15th September 2015

DOI: 10.1039/c5tc02405f

www.rsc.org/MaterialsC

The selective reduction of graphene oxide (GO) with direct laser writing is a rapid and efficient process to pattern conductive tracks for flexible electronic circuit applications. Here we report novel eye-friendly reduced graphene oxide (rGO) conductive tracks on transparent and flexible poly(ethylene terephthalate) (PET) substrates synthesized by one-step laser reduction of graphene oxide in an ambient environment. Resistivity as low as 1.07×10^{-4} μm has been achieved for a 20 nm thick rGO film after the industrial-grade 1064 nm Nd:YAG laser treatment. Fingerprints of the synthesized rGO were verified by Raman spectroscopy with an increased intensity ratio of the 2D band over the G band, and the deoxygenation results were examined using both X-ray photoelectron spectroscopy (XPS) and Fourier transform infrared (FTIR) characterization. The rGO synthesized by this infrared laser reduction showed increased absorption toward a shorter wavelength of up to 96% in UV regions, which can significantly protect human eyes from high energy light hazards. Electronic circuit tracks with rGO synthesized with this 1064 nm laser patterning process can provide novel methods for the fabrication of future eye-friendly flexible electronics with nonlinear optical transparency.

Introduction

Graphene is one of the most essential materials for next generation transparent and flexible electronics.[1] As a zero band gap material, the monolayer graphene has excellent conductivity.[2] With zero effective mass, it also possesses the highest mobility ever recorded.[3] Thus graphene has been intensively studied for various applications in emerging electronics, such as transistors, photo-detectors and solar cells.[4] Graphene can be synthesized by chemical vapour deposition (CVD), mechanical exfoliation from graphite, and reduction of graphene oxide. Using the CVD and mechanical exfoliation method we can synthesize high-quality single crystal graphene with almost no defects; however, the production rate is relatively small to satisfy the requirement of mass production.[5] Although the rGO synthesized using the modified Hummers method may include some defects, the low cost and high throughput features still make rGO feasible for mass production applications.[6]

Intensive studies have been focused on synthesizing rGO using photo deoxygenation methods during the past five years as summarized in Table 1. The KrF excimer laser with a wavelength of 248 nm and a pulse width of 20–25 ns was intensively investigated to reduce GO under H_2,[7] N_2,[8] water solutions,[9] and even in an ambient environment.[10] The ultrahigh energy of photons from the excimer laser can directly break the oxygen bonds attached to graphene, and can facilitate the reduction of GO to rGO. Meanwhile, the femtosecond laser possessing ultra-high photon energy within a short duration in the time-domain was also intensively studied to reduce GO. With the pulse width ranging from 100 to 120 fs, rGO was successfully synthesized using the femtosecond laser in both water solutions[11] and an ambient environment.[12–14] Simultaneously, the Nd:YAG laser at 1064 nm together with its second harmonic generation (SHG) and third harmonic generation (THG) lasers at 532 and 355 nm were also studied to reduce GO. With a short wavelength of 355 nm, the blue THG laser could effectively reduce GO in an ambient[15] and an N_2 environment[16] using a mechanism similar to the excimer laser. With a lower energy at 532 nm, the green SHG laser was still capable of reducing GO in an ambient/N_2 environment[16] and water solutions.[17] Using phase lock loops, the 1064 nm Nd:YAG with 10 picosecond pulse width can still synthesize rGO in an N_2 environment.[18] However, the fundamental 1064 nm with a pulse width of 7 ns did not show a significant reduction of GO in aqueous solution.[17] The possible mechanism is due to the high absorption of 1064 nm in water, so the photon energy may not be efficiently transferred into GO.[19]

Department of Industrial and Systems Engineering, The Hong Kong Polytechnic University, Hung Hom, Kowloon, Hong Kong. E-mail: mitch.li@polyu.edu.hk

Table 1 Summary for the laser reduction studies of GO

Wavelength (nm)	Pulse width	Duration	Environment	Reduction	Ref.
248	20 ns	20–100 pulses	50 mTorr H_2	Yes	7
248	25 ns	10–15 pulses	500 sccm N_2	Yes	8
248	20 ns	5 min	Water	Yes	9
248	20 ns	200 μm s^{-1}	Ambient	Yes	10
355	9 ns	20 s	Ambient/N_2	Yes	16
355	10 ns	10 s	Nil	Yes	20
355	10 ns	Nil	Ambient	Yes	15
532	7 ns	0–10 min	Water	Yes	17
532	9 ns/continuous	20 s	Ambient/N_2	Yes	16
788	Continuous	Nil	Ambient	Yes	21
790	120 fs	600 μs	Ambient	Yes	12 and 13
800	100 fs	1–400 pulses	Nil	Yes	22
800	120 fs	1–60 min	Water	Yes	11
800	120 fs	900 μs	Ambient	Yes	14
1064	10 ps	5–100 mm s^{-1}	N_2	Yes	18
1064	7 ns	0–2 min	Water	No	17

There have been increasing demands of flexible electronics for wearable devices, and the fabrication of low cost high quality conductive circuits is one bottleneck to supply these products.[20] However, there are few reports on the fabrication of flexible electronics based on low cost GO with the laser reduction using industrial-grade lasers in an ambient environment. The intensive studies for the reduction of GO using the excimer or femtosecond laser on GO may be rather expensive for practical applications in industry. Therefore it is crucial to develop industrial-grade laser reduction techniques for patterning graphene tracks on flexible substrates. PET is one of the most widely used plastic materials at the operating temperature below 250 °C.[21] Meanwhile, PET possesses ultralow transmittance at the near IR range and the adsorption at 1064 nm is 103 times lower than the widely used transparent indium tin oxide (ITO).[22] Meanwhile, graphene oxide has been proved to possess high absorption at the IR range.[23] Consequently, for a PET substrate coated with GO, infrared lasers can selectively interact with GO without affecting the properties of the underlying PET substrate.

Here the industrial-grade 1064 nm Nd:YAG laser reduction of GO on the PET substrate in an ambient environment was systemically investigated. The GO was first spin-coated on the transparent PET substrate, and then selectively reduced using an Nd:YAG laser in an ambient environment. The electrical resistivity was measured to be 1.07×10^{-4} Ωm determined by standard four-wire measurement. Porous rGO structures after the laser treatment were revealed by the scanning electron microscopy (SEM) characterization. Fingerprints of rGO were shown by the increased intensity ratio of the 2D band over the G band by Raman spectroscopy analysis. A dominant decrease of C═O bonds was proved by XPS and FTIR analysis. Optical transmittance results showed that these conductive rGO tracks synthesized by infrared laser treatment exhibited a larger absorption rate up to 96% towards higher energy lights. These nonlinear transparent and flexible electronic circuits fabricated by the proposed industrial-grade laser process can work as human eye-friendly filters against the hazards from high energy lights.

Experimental

rGO synthesis

GO aqueous solution was used as purchased from Graphene Laboratories Inc. NY, with over 60% as a monolayer, a concentration of 500 mg L^{-1} and a flake size ranging from 0.5 to 5.0 μm. The GO solution was spin-coated at 700 rpm on a 3M PET substrate for 60 s. Then the sample was heated at 95 °C for 30 min before laser treatment. A Lasertec Nd:YAG laser at 1064 nm with a repetitive rate of 5 kHz was used to reduce GO and the laser energy density was measured to be 150 mJ cm^{-2}. Circuit tracks were patterned on GO films by the computer-aided movement of the laser spot as illustrated in Fig. 1(a) and (b).

Materials characterization

The thickness of the GO film before and after the laser treatment was measured using a Wyko NT9000 optical profiling system with sub-nanometer resolution. The microstructures of GO and rGO samples were studied using a JEOL-5600LV SEM. The vibration modes of the GO and rGO were measured using a Renishaw 2000 × 50 confocal Raman spectrometer with 514 nm laser excitation. The resistivity of the rGO circuits was studied by standard four-wire measurement using an Agilent 4338B milliohmmeter. The chemical composition of GO before and after the laser treatment was characterized using an AXIS Ultra XPS from Kratos Analytical in the range of 1–1350 eV. Fourier transform infrared (FTIR) spectra were obtained using a Perkin-Elmer FTIR Multiscope Spectrum 100T spectrophotometer with KBr disks in the range of 500–4000 cm^{-1}. The UV-Vis transmittance of the rGO sample was characterized using a Perkin-Elmer LAMBDA 650 UV/Vis spectrophotometer ranging from 350 to 800 nm.

Results and discussion

Electrical resistivity

The as-prepared GO film on a PET substrate shows brown color as shown in Fig. 1(c) and the corresponding thickness of GO was measured to be 90 nm revealed by the optical profiler. After the laser writing, the patterned area shows grey color as shown

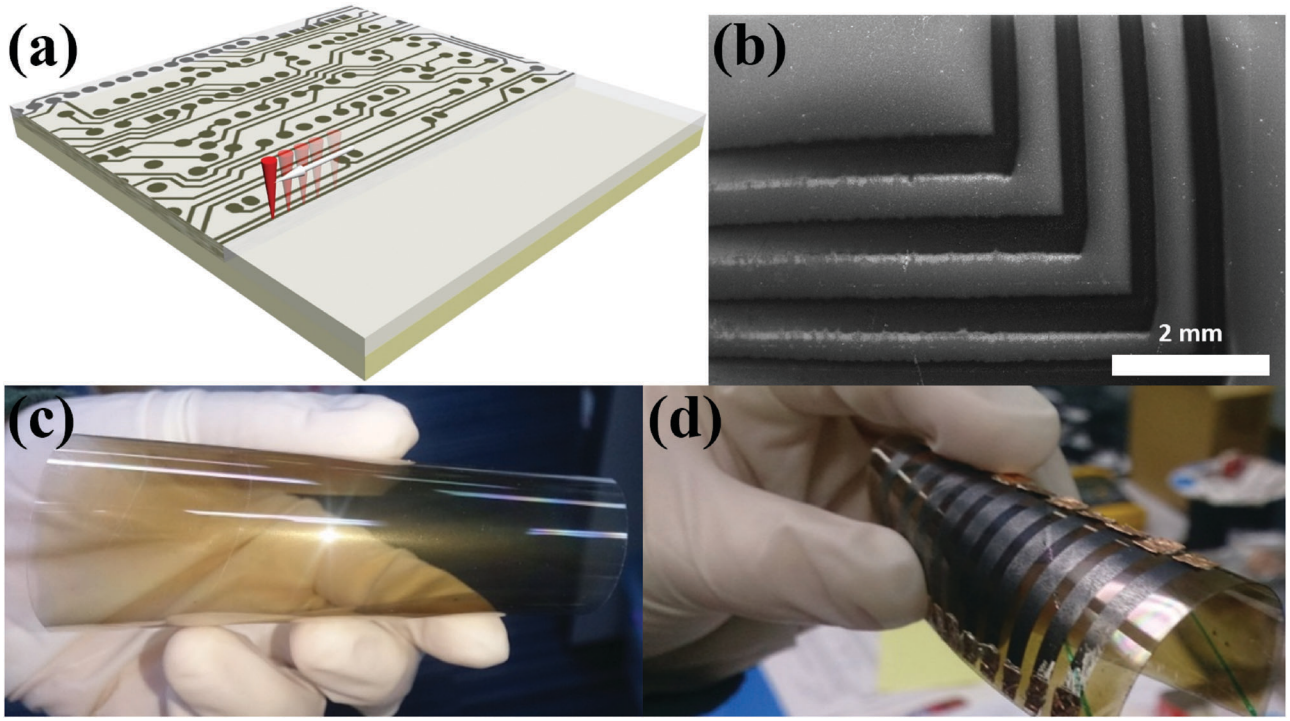

Fig. 1 (a) Schematic of GO reduction on a transparency sheet using an Nd-YAG laser. (b) SEM images of the patterned rGO circuits. The black regions represent rGO and the grey regions represent untreated GO. (c) GO spin coated on a transparent PET sheet before the laser reduction (d) the same sheet after the laser patterning as rectangular tracks to rGO.

in Fig. 1(d) and the thickness was reduced to 20 nm measured by the optical profiler. The resistivity of the laser patterned rGO was measured by standard four-wire measurement using conducting copper tapes as electrodes. The typical resistivity was measured to be 1.07×10^{-4} Ωm and 500 Ω sq^{-1} after 1064 nm laser reduction with an energy of 150 mJ cm^{-2}.

SEM characterization

The circuit tracks patterned by Nd:YAG laser were examined using SEM, as shown in Fig. 1(b). The grey color regions represent GO and the black color regions represent rGO. The higher resolution SEM images of GO before and after laser treatment are shown in Fig. 2 respectively. Smooth surfaces with higher folding boundaries due to the restacking of layers of GO are observed in GO, as shown in Fig. 2(a). This kind of morphology is uniform across large areas as illustrated in the zoom-out image in the inset of Fig. 2(a). After laser treatment, the surfaces of rGO become highly porous, as shown in Fig. 2(b). Grains are widely emerged across larger areas with crumpled and rippled structures, as shown in the zoom-out image in the inset of Fig. 2(b). The possible explanation of the morphology change might be due to the deoxygenation process during the laser treatment. rGO released oxygen and this reaction induced defects among the rGO. As a result, a porous surface was left after the laser reduction process.

Raman characterization

The fingerprints of GO before and after the 1064 nm laser treatment at energy density of 150 mJ cm^{-2} are identified by

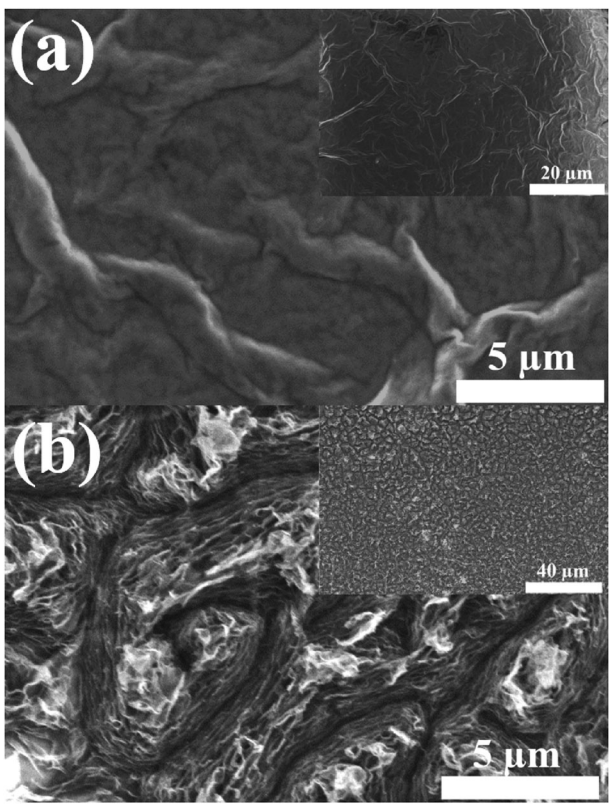

Fig. 2 SEM image of (a) GO before the laser reduction and (b) rGO after the laser reduction. The insets show the corresponding zoom-out images.

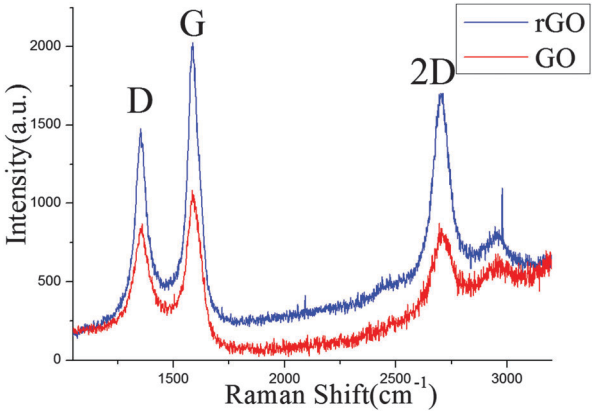

Fig. 3 Raman spectroscopy of the GO film before (red) and after the laser reduction (blue).

Raman spectroscopy with representative spectra as red and blue curves respectively in Fig. 3. The characteristic peaks at 1358, 1595, and 2691 cm^{-1}, corresponding to D, G, and 2D bands respectively, are used to recognize the GO and rGO. The G band at 1595 cm^{-1} represents the sp^3 hybridization of the carbon atoms in GO. The D and 2D bands both fit with symmetry Lorentzian curves. After laser reduction, the intensities of D and G bands are doubled. Meanwhile, the 2D intensity is increased up to 2.3 times after laser reduction. So the intensity ratio of the 2D band over the G band is increased, indicating more graphene is synthesized after the laser reduction.[24] Meanwhile, the full width at half maximum (FWHM) of the 2D peaks after Lorentzian fitting is 64 cm^{-1}. Previous work suggested that the 2D peak fitted with a single Lorentzian profile having a typical FWHM between 50 and 65 cm^{-1} could reveal the presence of turbostratic graphite,[16] which is composed of multiple randomly oriented graphene sheets.[25] To account for the crystalline quality of the GO films in terms of order parameters before and after laser-reduction, the mean domain sizes (L_a) in graphene, relating to the D/G intensity ratio, are used.[26,27] The empirical relation $L_a\,(nm) = 2.4 \times 10^{-10} \times \lambda_1^4 (I_D/I_G)^{-1}$ is re-examined, where λ_l is the probe laser wavelength (nm), I_D and I_G are the Raman area intensities of the D and G bands. From the red and blue spectrums in Fig. 3, L_a values of 18.8 nm and 28.2 nm were calculated for the un-reduced and the laser reduced GO. An increase in the L_a value suggests that the laser-reduced graphene oxide evolves to a more ordered state with fewer defects.[27] It can be inferred that the removal of oxygen atoms from GO films takes place without causing any damage to the lattice, which is consistent with the reported theoretical calculation results.[28]

XPS characterization

The chemical compositions of GO films before and after laser reduction are revealed by XPS spectra with curve fittings as shown in Fig. 4(a) and (b) respectively. The overall atomic ratios of oxygen to carbon are dramatically decreased from 3.8 to 0.09 after laser treatment, indicating dominant deoxygenation process occurred. The characteristic peaks at 284.5, 285.6, 287.2, and 289.0 eV correspond to C–C, C–O, C═O, and O–C═O

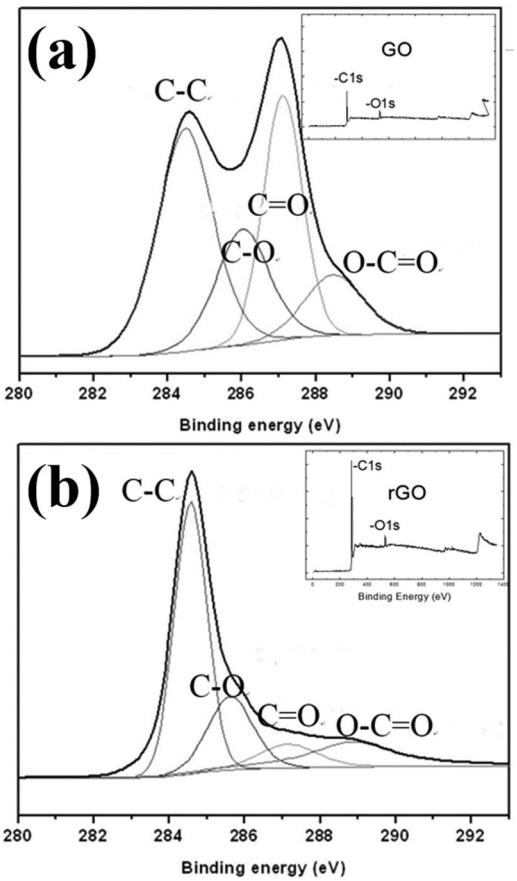

Fig. 4 XPS results and curve fittings of the GO film (a) before and (b) after the laser reduction. The two insets are the complete XPS spectrums ranging from 0 to 1350 eV.

functional groups respectively.[29–31] The intensity of the C–C bond at 284.5 eV shows similar orders of amplitude before and after the laser reduction, indicating that the carbon atoms in GO are not etched away during the laser reduction process. In comparison, the C–O bond at 285.6 eV and the O–C═O bond at 289.0 eV show a slight decrease after the laser treatment, indicating the less deoxygenation of these two bonds during the laser reduction process. The most significant decrease is found to be the C═O bond at 287.2 eV where the intensity is greatly reduced. Thus it can be inferred that the 1064 nm laser treatment is mainly deoxygenating the C═O bonds in GO.[32]

FTIR characterization

In order to further investigate the deoxygenation process after the laser reduction, the chemical components of the GO before and after the laser treatment were also studied using FTIR and shown in Fig. 5 as red and black curves respectively. Different types of oxygen containing functional groups on GO are observed at 3600 cm^{-1} (O–H stretching vibration), at 1720 cm^{-1} (C═O stretching vibration), at 1610 cm^{-1} (un-oxidized graphitic domain skeletal vibration), at 1230 cm^{-1}(C–OH stretching vibration) and at 1058 cm^{-1} (C–O stretching vibration).[33] The C═O stretching vibration peak at 1720 cm^{-1} is significantly smoothed after the

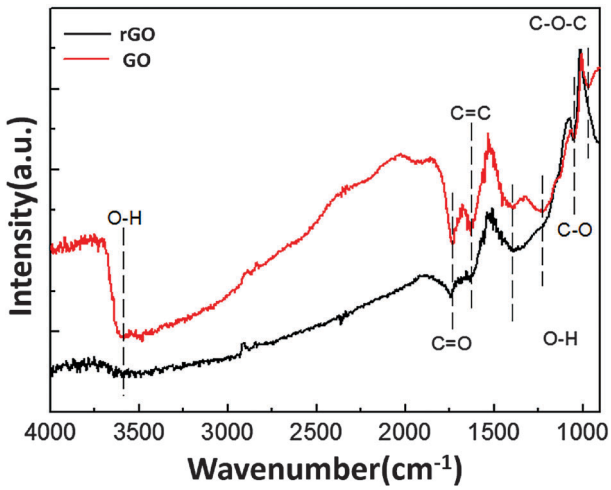

Fig. 5 FTIR results of the GO film before (red) and after (black) the laser reduction.

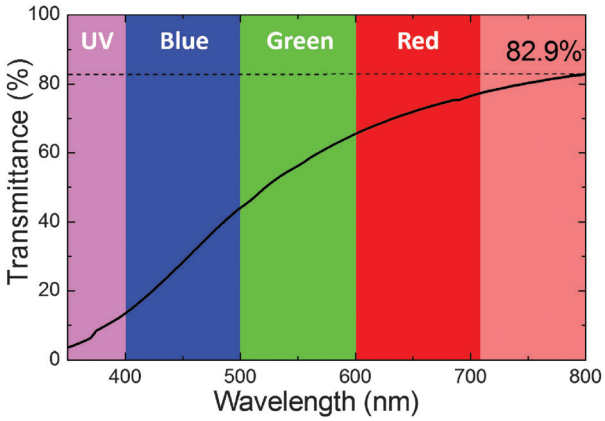

Fig. 6 UV-Vis transmittance spectrum of the rGO after the laser treatment.

laser treatment, indicating strong removal of C═O bonds by laser reduction. Meanwhile, the peaks of C–O and C–OH remained with similar amplitudes after the laser reduction. The characterization for the deoxygenation process by FTIR is consistent with the above XPS results. Significant amounts of C═O bonds are removed while fewer C–O and C–OH bonds are influenced, which may be due to the selective reduction of the current 1064 nm laser. During the laser treatment process, the absorption rates of GO exposed to different photon energies would be different. High energy lasers such as femtosecond or excimer lasers were reported to be more powerful to reduce the C–O bonds rather than C═O bonds.[7,8,13] In our case, the lower energy 1064 nm laser tends to selectively remove most of the C═O bonds rather than other bonds due to the smaller photon energy. So it can be deduced that the chemical components capable of absorbing high energy lights would remain after 1064 nm laser treatment. It may remarkably be a great advantage to use these conductive tracks as optical filters, which can critically absorb high energy lights including UV and blue lights.

Optical transmittance

In order to investigate the optical filtering effect for eye protection applications, the optical transmittance within the predominant reaching-earth solar spectrum (ranging from 350 to 800 nm) is measured on the rGO film by the laser treatment as shown in Fig. 6. As the photon energy increased, the absorption of the rGO film on PET increased dramatically from 17% at 800 nm to 96% at 350 nm. For low energy visible regions from 500 nm to 700 nm, the transmittance rate is increased from 40% to 75%, still revealing transparent features. At the high energy visible blue light region from 400 to 500 nm, the absorption rates are increased and all above 55%. For the UV region from 350 to 400 nm, the absorption rate is completely over 85%. So the laser treated rGO tracks show significant nonlinear absorption for high energy lights from 350 to 500 nm. There have been clinical studies reporting that exposure to UV light would cause disorders for human eyes.[34] Besides UV regions, it was found that patients with more exposures to high energy visible lights (400–500 nm) would also have more chances for developing age-related macular degeneration as suggested by clinical studies.[35] Accordingly, these rGO treated with 1064 nm laser would be excellent candidates to work as transparent electronic circuits as well as nonlinear long wavelength pass filters to protect human eyes from the harmful high energy lights. It is thus trustworthy that this kind of conductive rGO with such nonlinear transmittance at UV and visible ranges would become promising materials for emerging flexible and transparent electronics, especially for emerging wearable visual display devices.

Conclusions

Nonlinear optical transparent and electrical conductive rGO electronic circuits on flexible PET substrates were fabricated by a one-step laser reduction and patterning process in an ambient environment using an industrial grade 1064 nm Nd:YAG laser. The microstructures of the rGO after laser treatment showed significant porous structures as evinced by SEM. Dominant graphene synthesis was revealed by the increased 2D over G ratios in Raman spectroscopy. The deoxygenation process with significant removal of C═O bonds was verified by XPS and FTIR analysis. The resistivity of the laser reduced GO was measured to be as low as 1.07×10^{-4} Ωm. The UV-Vis spectrum of the laser treated rGO showed a nonlinear optical transparency with enhanced absorption as the photon energy increased. These selective transparency materials can efficiently reduce the hazards from high energy lights and protect human eyes from short-wavelength light radiation, which is crucial for future transparent and flexible electronics, especially for visual applications such as wearable displays and electronic glasses. Besides, this maskless laser direct patterning method is capable of structuring any arbitrary shapes drawn by computer-aided designs for the fabrication of patterns such as conductive tracks, resistors, and capacitors. Future work will include patterning rGO based electronic devices on other transparent substrates, such as polydimethylsiloxane (PDMS), for potential on-chip biomedical applications.

Acknowledgements

This work was funded by the Hong Kong Innovation Technology Fund (ITF) under Project No. ITS/041/14.

Notes and references

1 K. P. Loh, Q. L. Bao, P. K. Ang and J. X. Yang, *J. Mater. Chem.*, 2010, **20**, 2277–2289.
2 Y. Xu, K. Sheng, C. Li and G. Shi, *J. Mater. Chem.*, 2011, **21**, 7376–7380.
3 K. I. Bolotin, K. J. Sikes, Z. Jiang, M. Klima, G. Fudenberg, J. Hone, P. Kim and H. L. Stormer, *Solid State Commun.*, 2008, **146**, 351–355.
4 Y. Ye and L. Dai, *J. Mater. Chem.*, 2012, **22**, 24224–24229.
5 N. S. Safron and M. S. Arnold, *J. Mater. Chem. C*, 2014, **2**, 744–755.
6 Y.-Z. Liu, C.-M. Chen, Y.-F. Li, X.-M. Li, Q.-Q. Kong and M.-Z. Wang, *J. Mater. Chem. A*, 2014, **2**, 5730–5737.
7 V. Le Borgne, H. Bazi, T. Hayashi, Y. A. Kim, M. Endo and M. A. El Khakani, *Carbon*, 2014, **77**, 857–867.
8 D. A. Sokolov, C. M. Rouleau, D. B. Geohegan and T. M. Orlando, *Carbon*, 2013, **53**, 81–89.
9 L. Huang, Y. Liu, L. C. Ji, Y. Q. Xie, T. Wang and W. Z. Shi, *Carbon*, 2011, **49**, 2431–2436.
10 K. C. Yung, H. Liem, H. S. Choy, Z. C. Chen, K. H. Cheng and Z. X. Cai, *J. Appl. Phys.*, 2013, **113**, 244903.
11 H. W. Chang, Y. C. Tsai, C. W. Cheng, C. Y. Lin and P. H. Wu, *Electrochem. Commun.*, 2012, **23**, 37–40.
12 Y. L. Zhang, L. Guo, S. Wei, Y. Y. He, H. Xia, Q. D. Chen, H. B. Sun and F. S. Xiao, *Nano Today*, 2010, **5**, 15–20.
13 Y. G. Bi, J. Feng, Y. F. Li, Y. L. Zhang, Y. S. Liu, L. Chen, Y. F. Liu, L. Guo, S. Wei and H. B. Sun, *ACS Photonics*, 2014, **1**, 690–695.
14 H. Y. Chen, D. D. Han, Y. Tian, R. Q. Shao and S. Wei, *Chem. Phys.*, 2014, **430**, 13–17.
15 H. B. Jiang, Y. L. Zhang, D. D. Han, H. Xia, J. Feng, Q. D. Chen, Z. R. Hong and H. B. Sun, *Adv. Funct. Mater.*, 2014, **24**, 4595–4602.
16 D. A. Sokolov, K. R. Shepperd and T. M. Orlando, *J. Phys. Chem. Lett.*, 2010, **1**, 2633–2636.
17 V. Abdelsayed, S. Moussa, H. M. Hassan, H. S. Aluri, M. M. Collinson and M. S. El-Shall, *J. Phys. Chem. Lett.*, 2010, **1**, 2804–2809.
18 R. Trusovas, K. Ratautas, G. Raciukaitis, J. Barkauskas, I. Stankeviciene, G. Niaura and R. Mazeikiene, *Carbon*, 2013, **52**, 574–582.
19 E. J. G. Peterman, F. Gittes and C. F. Schmidt, *Biophys. J.*, 2003, **84**, 1308–1316.
20 A. Facchetti, *Nat. Mater.*, 2008, **7**, 839–840.
21 W. Cobbs and R. Burton, *J. Polym. Sci.*, 1953, **10**, 275–290.
22 S. Z. Xiao, S. A. Fernandes and A. Ostendorf, Lasers in Manufacturing 2011: Proceedings of the Sixth International Wlt Conference on Lasers in Manufacturing, Pt B, 2011, vol. 12, pp. 125–132.
23 M. Acik, G. Lee, C. Mattevi, M. Chhowalla, K. Cho and Y. J. Chabal, *Nat. Mater.*, 2010, **9**, 840–845.
24 X. Diez-Betriu, S. Alvarez-Garcia, C. Botas, P. Alvarez, J. Sanchez-Marcos, C. Prieto, R. Menendez and A. de Andres, *J. Mater. Chem. C*, 2013, **1**, 6905–6912.
25 D. R. Lenski and M. S. Fuhrer, *J. Appl. Phys.*, 2011, **110**, 013720.
26 L. G. Cancado, K. Takai, T. Enoki, M. Endo, Y. A. Kim, H. Mizusaki, A. Jorio, L. N. Coelho, R. Magalhaes-Paniago and M. A. Pimenta, *Appl. Phys. Lett.*, 2006, **88**, 163106.
27 A. C. Ferrari, *Solid State Commun.*, 2007, **143**, 47–57.
28 H. Zhang and Y. Miyamoto, *Phys. Rev. B: Condens. Matter Mater. Phys.*, 2012, **85**, 033402.
29 Z. J. Fan, W. Kai, J. Yan, T. Wei, L. J. Zhi, J. Feng, Y. M. Ren, L. P. Song and F. Wei, *ACS Nano*, 2011, **5**, 191–198.
30 H. R. Byon, J. Suntivich and Y. Shao-Horn, *Chem. Mater.*, 2011, **23**, 3421–3428.
31 K. R. Lee, K. U. Lee, J. W. Lee, B. T. Ahn and S. I. Woo, *Electrochem. Commun.*, 2010, **12**, 1052–1055.
32 C. J. Fu, G. G. Zhao, H. J. Zhang and S. Li, *Int. J. Electrochem. Sci.*, 2014, **9**, 46–60.
33 Y. X. Xu, H. Bai, G. W. Lu, C. Li and G. Q. Shi, *J. Am. Chem. Soc.*, 2008, **130**, 5856–5857.
34 O. Hockwin, M. Kojima, Y. Sakamoto, A. Wegener, Y. B. Shui and K. Sasaki, *J. Epidemiol.*, 1999, **9**, 39–47.
35 H. R. Taylor, S. West, B. Munoz, F. S. Rosenthal, S. B. Bressler and N. M. Bressler, *Arch. Ophthalmol.*, 1992, **110**, 99–104.